



## Predicting changes in renal metabolism after compound exposure with a genome-scale metabolic model



Kristopher D. Rawls<sup>a</sup>, Bonnie V. Dougherty<sup>a</sup>, Kalyan C. Vinnakota<sup>b,c</sup>, Venkat R. Pannala<sup>b,c</sup>, Anders Wallqvist<sup>b</sup>, Glynis L. Kolling<sup>a,d</sup>, Jason A. Papin<sup>a,d,e,\*</sup>

<sup>a</sup> Department of Biomedical Engineering, University of Virginia, Charlottesville, VA 22908, USA

<sup>b</sup> Department of Defense Biotechnology High Performance Computing Software Applications Institute, Telemedicine and Advanced Technology Research Center, U.S. Army Medical Research and Development Command, Fort Detrick, MD 21702, USA

<sup>c</sup> Henry M. Jackson Foundation for the Advancement of Military Medicine, Inc. (HJF), Bethesda, MD 20817, USA

<sup>d</sup> Department of Medicine, Division of Infectious Diseases and International Health, University of Virginia, Charlottesville, VA 22908, USA

<sup>e</sup> Department of Biochemistry & Molecular Genetics, University of Virginia, Charlottesville, VA 22908, USA

### ARTICLE INFO

#### Keywords:

Kidney  
Kidney Metabolism  
Metabolic Modeling  
Nephrotoxicity  
Transcriptomics  
Metabolomics

### ABSTRACT

The kidneys are metabolically active organs with importance in several physiological tasks such as the secretion of soluble wastes into the urine and synthesizing glucose and oxidizing fatty acids for energy in fasting (non-fed) conditions. Once damaged, the metabolic capability of the kidneys becomes altered. Here, we define metabolic tasks in a computational modeling framework to capture kidney function in an update to the *iRno* network reconstruction of rat metabolism using literature-based evidence. To demonstrate the utility of *iRno* for predicting kidney function, we exposed primary rat renal proximal tubule epithelial cells to four compounds with varying levels of nephrotoxicity (acetaminophen, gentamicin, 2,3,7,8-tetrachlorodibenzodioxin, and trichloroethylene) for six and twenty-four hours, and collected transcriptomics and metabolomics data to measure the metabolic effects of compound exposure. For the transcriptomics data, we observed changes in fatty acid metabolism and amino acid metabolism, as well as changes in existing markers of kidney function such as *Clu* (clusterin). The *iRno* metabolic network reconstruction was used to predict alterations in these same pathways after integrating transcriptomics data and was able to distinguish between select compound-specific effects on the proximal tubule epithelial cells. Genome-scale metabolic network reconstructions with coupled omics data can be used to predict changes in metabolism as a step towards identifying novel metabolic biomarkers of kidney function and dysfunction.

### 1. Introduction

The kidneys are vital organs responsible for many functions such as filtering blood, regulating water and electrolyte balance, and filtering waste from the body (Onopiu et al. 2015; Scott and Quaggia 2015). Metabolism is a key biochemical process in the performance of these functions by (1) generating energy for filtering and reabsorbing metabolites back into the blood, and (2) breaking down fatty acids, amino acids, and other metabolites to be used by other organs (Weidemann and Krebs 1969; Bobulescu 2010). The kidneys can sustain consistent injury before a loss of function is observed, typically measured by increases in creatinine or urea to diagnose damage that has occurred (Bellomo et al. 2012). Understanding the genesis and progression of these diseases

could be useful in investigating prevention or treatment strategies that mitigate damage or help restore kidney function, respectively.

Computational models can be used to interrogate how a disease or specific condition affects kidney function. Computational models can simulate a biological system of interest to understand how perturbations change system dynamics (Waikar and Bonventre 2009; Layton 2013; Sgouralis and Layton 2015). Genome-Scale Network REconstructions (GENREs) provide a mathematical framework to represent the biochemical reactions and metabolites of a cell or organism to depict its metabolism (Rawls, Dougherty, et al. 2019). GENREs have been used to represent metabolism of microbial species (Orth et al. 2011; Bartell et al. 2017; Carey et al. 2017) and more recently to represent global changes in human and rat metabolism (Mardinoglu et al. 2014; Blais et al. 2017).

\* Corresponding author at: Department of Biomedical Engineering, Box 800759, Health System, University of Virginia, Charlottesville VA 22908, USA.  
E-mail address: [papin@virginia.edu](mailto:papin@virginia.edu) (J.A. Papin).

These network reconstructions can be adapted to capture tissue or cell-type specificity to address key questions about underlying biological mechanisms or changes in phenotypes. To date, there have been few models developed to represent kidney metabolism (Chang et al. 2010; Zhang et al. 2013; Sohrabi-Jahromi et al. 2016). However, these models are based on a previous reconstruction that has since been updated to capture more metabolic pathways, metabolites and reactions (Thiele et al. 2013; Swainston et al. 2016). Also, these models were focused on predicting drug effects, or focal segmental glomerulosclerosis (FSGS), and do not directly address drug toxicity, thus motivating a new application of a model of kidney metabolism.

It is possible to experimentally measure the changes in levels of metabolites in the blood or urine to assess the degree of damage that has occurred in damaged kidney tissue. Traditional measures of declining kidney function include measuring serum creatinine clearance (Himelfarb and Ikizler 2007) and blood urea nitrogen (Gowda et al. 2010); however, these markers change under many conditions and are not limited to just kidney-specific injury, highlighting the need for new biomarkers of kidney function to properly assess damage (Kim and Moon 2012). New protein biomarkers have been discovered (Dieterle et al. 2010; Adiyanti and Lohr 2012; Bonventre 2014), but have shown inconsistent results in human studies (Endre et al. 2011; de Geus et al. 2012). One way to discover potential biomarkers is with the use of omics profiling data (Connor et al. 2010; Blanchet et al. 2011; Mattheis et al. 2011; Zierer et al. 2015). Transcriptomics and metabolomics data are useful for characterizing global changes in mRNA expression and metabolite levels. Omics data have been used with GENREs to make predictions on how metabolism is altered after compound exposure (Agren et al. 2014; Stempler et al. 2014; O'Brien et al. 2015; Blais et al. 2017; Sawada et al. 2018; Rawls, Blais, et al. 2019).

Here, we (a) present an updated, rat network reconstruction (*iRno*) that has been expanded to include kidney function, (b) collect and analyze paired transcriptomics and metabolomics data from compound-treated kidney cells, and (c) make predictions of changes in metabolite levels after compound exposure. The updated *iRno* reconstruction contains changes to existing biochemical reactions and the addition of several hundred new reactions. We also exposed primary rat renal proximal tubule epithelial cells (RPTECs) to four different compounds with varying effects on metabolism after six and 24-h. From this experiment, we collected paired transcriptomic and metabolomic data to characterize the response of the RPTECs to the different compounds. Lastly, we combined the transcriptomics data with *iRno* using the Transcriptionally Inferred Metabolite Biomarker Response (TIMBR) algorithm (Blais et al. 2017) to predict changes in metabolite levels based on the control and treatment conditions. Metabolites that change between the two groups could potentially serve as biomarkers prior to kidney injury. With this approach, we provide an updated GENRE expanded to include kidney-specific functionality, as well as a framework for determining novel, extracellular biomarkers produced in response to compounds of interest.

## 2. Methods

### 2.1. Creation of kidney-specific metabolic tasks

Metabolic tasks are reactions or pathways that ensure the conversion of one metabolite to another, representing the known biological function of the organism or cell of interest. Here, metabolic tasks were created by reviewing the literature on rat kidney function, and more specifically RPTECs. Tasks were first taken from the previously published *iRno* model that represented overlapping functions between the liver and the kidney. Next, literature was reviewed and tasks were added that came from published data on functions that occur in the rat kidney. Overall, a total of 155 tasks was created and has been used in a previous publication (Pannala et al. 2019).

### 2.2. Flux balance analysis and the expansion of *iRno*

To expand the *iRno* network reconstruction to more completely capture kidney metabolic function, the literature was searched to find evidence of reactions known to occur but not previously captured in the model. Additionally, metabolites and reactions were added to *iRno* that allow the model to secrete metabolites detectable in plasma. The list of changes to *iRno* are summarized in Supplementary Data 6 resulting in the addition of two new metabolites, 87 metabolites that were newly assigned to different compartments, four new reactions, 89 transport reactions to bring metabolites into their newly assigned compartments, and 193 exchange reactions. *iRno* now accounts for the function of 5716 metabolites and 8532 reactions. A new metabolic objective function was created based on the previous biomass objective (Blais et al. 2017), excluding bile acids. Gluconeogenesis was also used as an objective function since the kidneys synthesize a considerable amount of glucose for the body (Gerich et al. 2001). To simulate gluconeogenesis, glutamine, lactate, and glycerol are used as inputs, and glucose was used as an output. These two objective functions were explored independently to interrogate kidney function. Flux balance analysis was used to simulate the flux through individual reactions using the cobra toolbox v.2.0.6 (Schellenberger et al. 2011) for MATLAB 2016b.

### 2.3. Renal proximal tubule epithelial cell growth conditions

Primary Renal Proximal Tubule Epithelial Cells (RPTECs) isolated from 10 week old, female Sprague-Dawley rats (RA-6015, Lot #F062414W10; Cell Biologics; Chicago, IL) were grown on gelatin-coated wells using DMEM:F12 supplemented with penicillin/streptomycin, L-glutamine, 5% FBS, ITS (insulin-transferrin-selenium) and epidermal growth factor (EGF; 100 µg/mL) without phenol red. Media and supplements were purchased from Gibco/Thermo-Fisher or supplied with cells purchased from Cell Biologics. RPTECs were plated at a density of 200,000 cells/well in a 12-well plate (Thermo-Fisher) and cultured overnight (90–95% confluence) prior to compound exposure.

### 2.4. RPTEC exposure conditions

RPTECs were exposed to compounds (Sigma Aldrich) at sub-toxic concentrations with DMSO (0.1%) as the vehicle control (Supplemental Fig. 1). The compounds and concentrations selected were acetaminophen (APAP) at 10 mM, gentamicin (GENT) at 10 mM, 2,3,7,8-tetrachlorodibenzodioxin (TCDD) at 1 nM, and trichloroethylene at 1 mM. The concentrations and time points were selected based on previous concentrations for similar studies in rat, human, and mouse kidney cells (Smith 1988; Boogaard et al. 1989; Mugford 1997; Lash et al. 2001; Robbiano et al. 2004; Dong et al. 2010; Vrbová et al. 2016) and viability measures (Supplemental Fig. 1; RealTime-Glo MT Cell Viability assay; Promega, Madison, WI). The results presented in this paper are part of a larger project examining the metabolic responses of multiple cell lines, including primary hepatocytes and cardiomyocytes. Compounds in the larger study were selected to cover both intentional exposures (e.g. pharmaceuticals: acetaminophen, gentamicin) and unintentional exposures (e.g. environmental: TCE, TCDD) with the goal of tracking cell-type specific metabolic response(s) using paired transcriptomics and metabolomics data. While gentamicin is a primary nephrotoxicant, there is evidence to suggest nephrotoxic effects from APAP and TCE (Newton et al. 1983; Cojocel et al. 1989; Mazer and Perrone 2008). TCDD is hepatotoxic (Boverhof et al. 2006; Bentli et al. 2013) and was included in our experiments for comparison to previously published data and to differentiate its effects from compounds known to preferentially affect the kidney.

### 2.5. RNA isolation, sequencing, and analysis

RPTECs were exposed to the compounds mentioned above with three

wells per compound or vehicle control. After exposure, cells from individual wells were lysed with Trizol to begin RNA extraction. Cell lysates were spun with chloroform in phase-lock gel tubes inside a cold room and the upper phase was then decanted into new tubes. Isopropanol and glycogen were added to the mixture and spun again resulting in an RNA pellet, which was washed with 75% ethanol twice. DNA was removed with a kit (Ambion/Invitrogen) and then RNA was quantified. rRNA was then depleted and mRNA was sent to a core facility ([med.virginia.edu/gatc/about/](http://med.virginia.edu/gatc/about/)) for library construction and sequencing. RNA was sequenced in a 2x125bp pair-end (PE) configuration and fastq files were generated. Kallisto v 0.43.0 (Bray et al. 2016) was used to process raw fastq files to quantify transcript abundances in transcripts per million (TPM) under default settings. Transcript abundances were then aggregated to the gene level in R v. 3.5.1 with the package tximport (Soneson et al. 2015), and differential gene expression was calculated with DESeq2 (Love et al. 2014) with a significance threshold at FDR < 0.1.

## 2.6. Gene enrichment analysis

To further analyze the differentially expressed genes, we used the R package clusterProfiler (Yu et al. 2012) to find KEGG pathways that were enriched. Differentially expressed genes for each condition and time point were first sorted into lists of Entrez Gene ID numbers. Next, the list of Entrez Gene ID numbers was passed through the command enrichKEGG to find the relevant pathways in the KEGG database that were enriched. Pathways were considered enriched with an adjusted  $p < 0.05$ .

## 2.7. Metabolomics

After RPTECs were exposed to compounds for six or 24 h, the spent media (extracellular media) was collected, frozen, and shipped to West Coast Metabolomics at the University of California, Davis (<http://metabolomics.ucdavis.edu/>) for metabolomics analysis by their Core Facilities. At West Coast Metabolomics, samples were processed for untargeted analysis of primary metabolites by Gas Chromatography Mass Spectrometry (GC-MS), analysis of complex lipids via Liquid Chromatography Mass Spectrometry (LC-MS), and biogenic amines through Hydrophilic Interaction Chromatography Quadrupole Time of Flight (HILIC-QTOF) Mass Spectrometry. Both external and internal standards for quality control were prepared and analyzed along with individual samples.

Primary metabolites were analyzed using a previously published protocol (Fiehn 2016) and results were reported by the relative peak intensities at the specified mass/charge retention index. For lipid analysis, samples were prepared with methanol, methyl tert-butyl ether (MTBE), and water before running LC-MS; peak intensities were reported following a published protocol (Cajka and Fiehn 2017). Biogenic amines were prepared by separating polar hydrophilic small molecules from lipids, according to a previously established method (Matyash et al. 2008), and raw peak intensities were then reported from analyzed samples using previously published protocols (Meissen et al. 2015). Relative peak intensities of identified and unidentified metabolites were generated together. Peak intensities were normalized and then analyzed by background subtraction, log transformation, centering the data around zero, and then Pareto-scaled within each metabolite. Normalized values were then subtracted from the fresh media samples to give a direction of change, either consumption or production. Data analysis was performed using R v 3.5.1. Metabolites were considered changed from control with statistical significance if  $p$ -values from the Kruskal-Wallis test, run in the FSA package (Ogle et al. 2019), were below a defined threshold ( $p < 0.05$ ).

## 2.8. TIMBR algorithm

The TIMBR algorithm (Blais et al. 2017) uses transcriptomics data

and a GENRE to make predictions on the relative production levels of metabolites. Default weights are assigned to each reaction based on the type of reaction it is (biochemical, boundary, transport, etc.). For reactions associated with differentially expressed genes, the log2fold changes are then multiplied by default reaction weights to get the final reaction weights. Raw production scores for control and treatment conditions were calculated by minimizing the sum of the product of the final reaction weights and flux through each reaction, across all reactions. Production scores for the control condition and the treatment condition were then combined using the previously described formula (Blais et al. 2017) to determine the relative production of a metabolite. These production scores were then z-transformed and used for downstream analyses. A full description of the method is available (Blais et al. 2017) and the source code to run the algorithm can be found on github ([www.github.com/csbl/ratcon1](https://www.github.com/csbl/ratcon1)).

## 3. Results

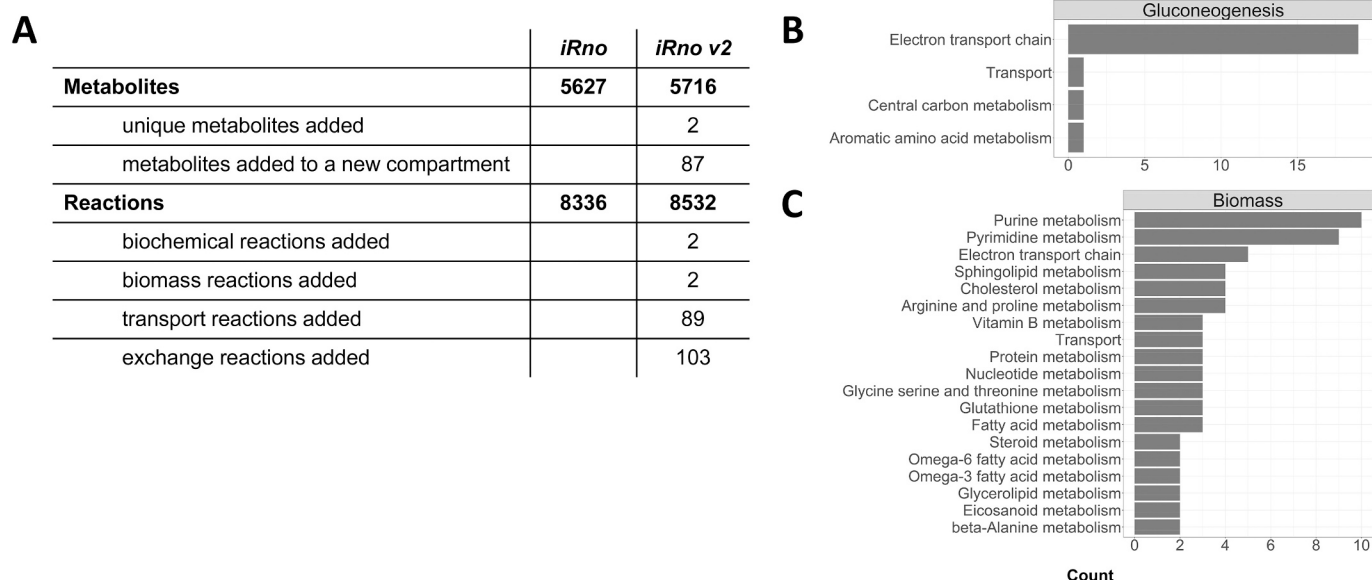
### 3.1. Updating iRno to reflect kidney-specific metabolic function

We expanded *iRno* by reviewing literature for evidence of metabolic reactions we had not yet captured and added metabolites that participated in these reactions. One reaction was the L-glutamate:2-aminobutanoate gamma-ligase reaction, converting glutamate and (S)-2-aminobutyanoate to  $\gamma$ -L-glutamyl-L-alpha-aminobutyrate. Another reaction was the conversion of gamma-L-L-glutamyl-L-alpha-aminobutyrate to ophthalmate, which was previously confirmed as a by-product of glutathione metabolism (Soga et al. 2006). Additionally, we also found evidence of metabolites that were detected in the plasma, so we updated *iRno* to reflect this change. To incorporate the secretion of the new metabolites, we added transport reactions to move metabolites from the cytosol to the extracellular compartment, as well as exchange reactions to move the metabolites from the extracellular compartment to the external environment. This curation effort resulted in the addition of 89 metabolites, 196 reactions, and 11 changes to existing reactions (Fig. 1A).

We created a new biomass equation that was derived from the previously published biomass equation for *iRno* (Blais et al. 2017) with the removal of bile acid-related terms given their specificity to hepatocyte function which was the focus of the previous work. For kidney-specific functionality, we also tested gluconeogenesis from lactate, glutamine, and glycerol as objective functions using previously defined physiological constraints (Elhamri et al. 1993; Pannala et al. 2019). After exploring biomass and gluconeogenesis as objective functions, we simulated gene knockouts to determine genes that are required for flux through both of these reactions. This analysis generated a list of genes that are necessary to be active for biomass and glucose to be produced. Removing bile acids from the biomass equation resulted in the removal of 16 genes from the list of genes required to achieve flux through the biomass equation (Fig. 1). For gluconeogenesis, 20 genes were required to be active for glucose to be synthesized from lactate, glutamine, and glycerol. It was interesting to note that none of the reactions associated with these genes were required to carry flux to produce biomass. The difference in required active genes for biomass and gluconeogenesis demonstrates the range of function captured with the reconstruction. Once we finished expanding *iRno*, we used the model to predict how kidney metabolism would be altered after compound exposure.

### 3.2. Transcriptomics recapitulate known kidney-specific response to compound exposure

After exposing renal proximal tubule epithelial cells (RPTECs) to Acetaminophen (APAP), Gentamicin (Gent), 2,3,7,8-tetrachlorodibenzo-dioxin (TCDD), and Trichloroethylene (TCE) for six and twenty-four hours, we measured the cell's response at the mRNA level. Table 1 provides a list of the number of differentially expressed genes from each

**Fig. 1.** Summary of changes to *iRno*.

Model statistics from the first version of *iRno* to this update termed *iRno v2* (A) The number of additions and changes for metabolites and reactions are displayed. Bar charts show the subsystem classification from the model of the genes that are required for (B) gluconeogenesis and (C) biomass.

**Table 1**

Differentially expressed gene counts from proximal tubule epithelial cells after exposure to APAP, Gent, TCDD, and TCE for six and twenty-four hours. Each treatment condition is compared to DMSO controls.

Chemical Compound	Number of differentially expressed genes (FDR < 0.1)	Number of differentially expressed genes (FDR < 0.1) accounted for in the <i>iRno</i> reconstruction
APAP – 6 h	7446	1003
APAP – 24 h	8797	1212
Gent – 6 h	2667	361
Gent – 24 h	8770	1157
TCDD – 6 h	3	0
TCDD – 24 h	9548	1269
TCE – 6 h	7	1
TCE – 24 h	6543	924

condition and time point. The third column shows the number of differentially expressed genes that we consider to be metabolic, mapping to genes accounted for in *iRno*. A summary of changes for metabolic genes is displayed in Fig. 2. Within each condition, the highest number of DEGs was seen at 24 h. We also noticed that several genes changed similarly in the 24-h condition (Fig. 2) so we decided to take a further look. A full list of gene expression changes is shown in Supplementary Data 1. There were 370 genes upregulated, and 258 genes downregulated across the APAP, TCDD, Gent, and TCE conditions. Among this group were genes related to amino acid synthesis such as *Asns*, and *Thns1l*, as well as amino acid transport into the cell like *Slc7a5*, *Slc16a10*, and *Slc16a17*. In addition to amino acid metabolism, genes relating to fatty acid metabolism were also increased. This includes genes related to fatty acid elongation including *Elovl4*, *Elovl5*, and *Acs1l*. Among the downregulated genes, several are involved in mitochondrial processes, such as cytochrome c oxidase (*Cox6c*, *Cox6b1*), and NADH dehydrogenase (*Mt-nd5*, *Mt-nd3*, *Mt-nd1*), which suggests an alteration in energy production in the cell. The upregulation of fatty acids and amino acid processes highlights the importance of these two pathways in kidney metabolism.

While exploring the results from the transcriptomics data, we also looked at specific genes that map to enzymes known to be markers of kidney injury to validate that we see intoxication at our chosen concentrations. Clusterin (*Clu*) is a biomarker of acute kidney injury in rats

(Vaidya et al. 2008) and is known to have a cytoprotective role in the kidney, although these mechanisms are not well understood (Ngan et al. 2014). We observed increased differential expression in the 24-h conditions for APAP, Gent, TCDD, and TCE, as well as the six-hour condition for APAP. This increase suggests that the RPTECs are undergoing some form of injury response after compound exposure at the concentrations we tested. We saw an increase in Lipocalin 2 (*Lcn2*) expression in TCE and TCDD at 24 h, but a decrease in the APAP and Gent conditions. Decreased expression in APAP treated cells would be expected given that *Lcn2* is an inflammatory marker and APAP acts to inhibit inflammation. Additional markers that have been utilized to assess kidney injury include: netrin (*Ntn1*),  $\beta$ -2-microglobulin (*B2m*), IL-18 (*Il18*), and cystatin C (*Cst3*) (Griffin et al. 2019). While a consistent universal response across these genes was not apparent, compounds did elicit a response. For *Ntn1*, we see increased gene expression for APAP (6 and 24 h), TCDD (24 h) and TCE (24 h). For *B2m*, we see increased gene expression for Gent, TCDD, and TCE at 24 h. For *Il18*, we see decreased gene expression for Gent and TCDD at 24 h. Finally, for *Cst3*, we see increased gene expression for APAP (6 h), TCDD (24 h) and TCE (24 h). Notably, increases in kidney injury marker (Kim-1) were not detected within spent media or at the expression level possibly due to the sub-toxic levels of compounds under study or the *in vitro* system (Luo et al. 2016). Together, changes in these biomarkers suggest a unique but injurious response for each compound. We were able to identify trends consistent with the literature on the expression of particular biomarkers related to kidney injury and confirm that exposure to these compounds at our chosen concentrations significantly perturbs metabolism of the RPTECs. Next, we next wanted to identify common pathways enriched as a result of compound exposure.

### 3.3. Pathways enriched from compound exposure

Using the data for metabolic genes differentially expressed in each condition, we examined enriched pathways using the clusterProfiler R package (Yu et al. 2012) to identify any general or condition-specific responses of the RPTECs to treatment. Supplementary data 2 contains a list of enriched pathways for each condition. The oxidative phosphorylation pathway was enriched in APAP, TCDD, and TCE conditions at 24 h. In the TCE 24-h condition, genes in this pathway were decreased, suggesting an impairment in the production of energy. In the

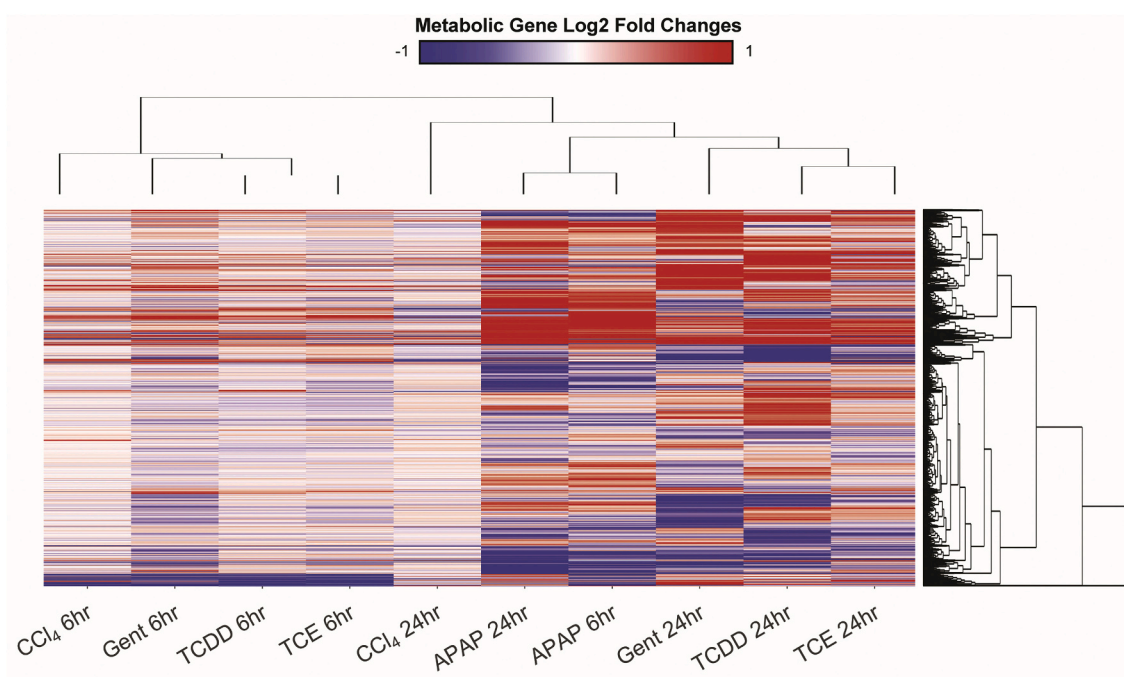


**Fig. 2.** Gene expression changes in response to toxicant exposure.

The heatmap above shows the fold changes for differentially expressed genes that can be found within the *iRno* model for any gene that was significant in at least 1 of the 10 conditions. Blue shows log<sub>2</sub> fold changes less than 0 (downregulated) while red shows log<sub>2</sub> fold changes greater than 0 (upregulated). Genes are clustered using Euclidean distance and with complete linkage, while conditions are clustered using the distance of Spearman correlations, with complete linkage

APAP and TCDD 24-h conditions, there was a mix of responses with some portions of the pathway upregulated and other portions downregulated. While oxidative phosphorylation is necessary for energy production given the demands of active transport of the kidney, reactive oxygen species are produced, and this increase in ROS production contributes to the oxidative stress of the RPTECs after exposure (Baud and Ardaillou 1986; Ratliff et al. 2016). Pathways associated with lipid and fatty acid metabolism were enriched in most conditions (Fig. 3), signifying that alteration of fatty acid metabolism could be a common response of the kidney cells to various compound exposure(s). Pathways associated with branched-chain amino acid metabolism were enriched in the APAP condition at both time points, as well as Gent and TCDD at 24 h. In the APAP 24-h condition, the aldosterone-regulated sodium regulation pathway was enriched, while in Gent the ATP-binding cassette transporter pathway was enriched. Both of these pathways are important to kidney metabolism and transport function, as ATP is needed to transport metabolites across the membrane, while aldosterone can trigger the reabsorption and excretion of sodium and water (Spitzer 1982). At the pathway level, we observed that energy metabolism, amino acid metabolism, and fatty acid/lipid metabolism were enriched across all categories suggesting that these are key metabolic processes altered by compound exposure. The ability of kidney cells to uptake or secrete amino acids, glucose, or fatty acids could be indicative of kidney dysfunction. From this result, we next wanted to independently look at the metabolomics data and see which metabolites and pathways were altered and how the pathways identified as different with the metabolomics data compare to pathways that were enriched as identified in the transcriptomics data.

#### 3.4. Metabolomics data recapitulate that compounds cause oxidative stress on renal proximal tubule epithelial cells

We computed the total number of detected metabolites that were statistically changed for each condition (Table 2), comparing all conditions against each other and discovered that APAP exposure at six and 24 h resulted in the most differentially changed metabolites among the

four compounds, while Gent and TCDD exposure at six hours produced the next largest change. Metabolite data were normalized and summarized as presented in Fig. 4. Each identified metabolite, for which there was a statistically significant change with respect to blank or control, is shown in the plot, with the RPTECs exposure condition on the x-axis, and the normalized metabolite levels on the y-axis. The measured metabolite abundances in blank media were subtracted from each condition in Fig. 4 to demonstrate direction of change, where positive values indicate a metabolite has been produced and negative values indicate a metabolite was consumed. Raw data are reported along with DMSO controls in the Supplementary Data 3 file.

Across all conditions, 16 identified metabolite levels are changed with statistical significance from the control condition. Of these 16 metabolites, 7 are amino acids. Within the amino acids, we see unique consumption of cysteine in the TCE six-hour condition, unique production of histidine and consumption of tryptophan in the APAP six-hour condition and unique production of ornithine in the TCDD six-hour condition. However, in the 24-h conditions, we see production of glycine for the APAP, Gent, and TCDD conditions. In contrast to the six-hour condition, we see consumption of histidine in the APAP condition and production of valine in the TCDD condition. Together, these results suggest a unique role for amino acids in response to toxicity.

3,6-anhydro-D-galactose is a metabolite produced from D-galactose, which is in the polysaccharide porphyrin. Porphyrin has been shown to have antioxidant effects that protect the kidneys from oxidative stress (Wang et al. 2017). Given that we see increases in 3,6-anhydro-D-galactose in the supernatant at the six-hour timepoint for both APAP and Gent, we can hypothesize that there was galactose catabolism *in vitro* in the RPTECs in an effort to maintain homeostasis by protecting against the oxidative stress resulting from acetaminophen and gentamicin-exposure (Weinberg et al. 1980; Weinberg and Humes 1980; Banday et al. 2008; Narayana 2008; Canayakin et al. 2016). Overall, the metabolomics data show the changes in metabolism associated with oxidative stress and amino acid metabolism. To investigate further, we looked at the transcriptomics data and metabolomics data together to see if there were consistent changes between the datasets we could

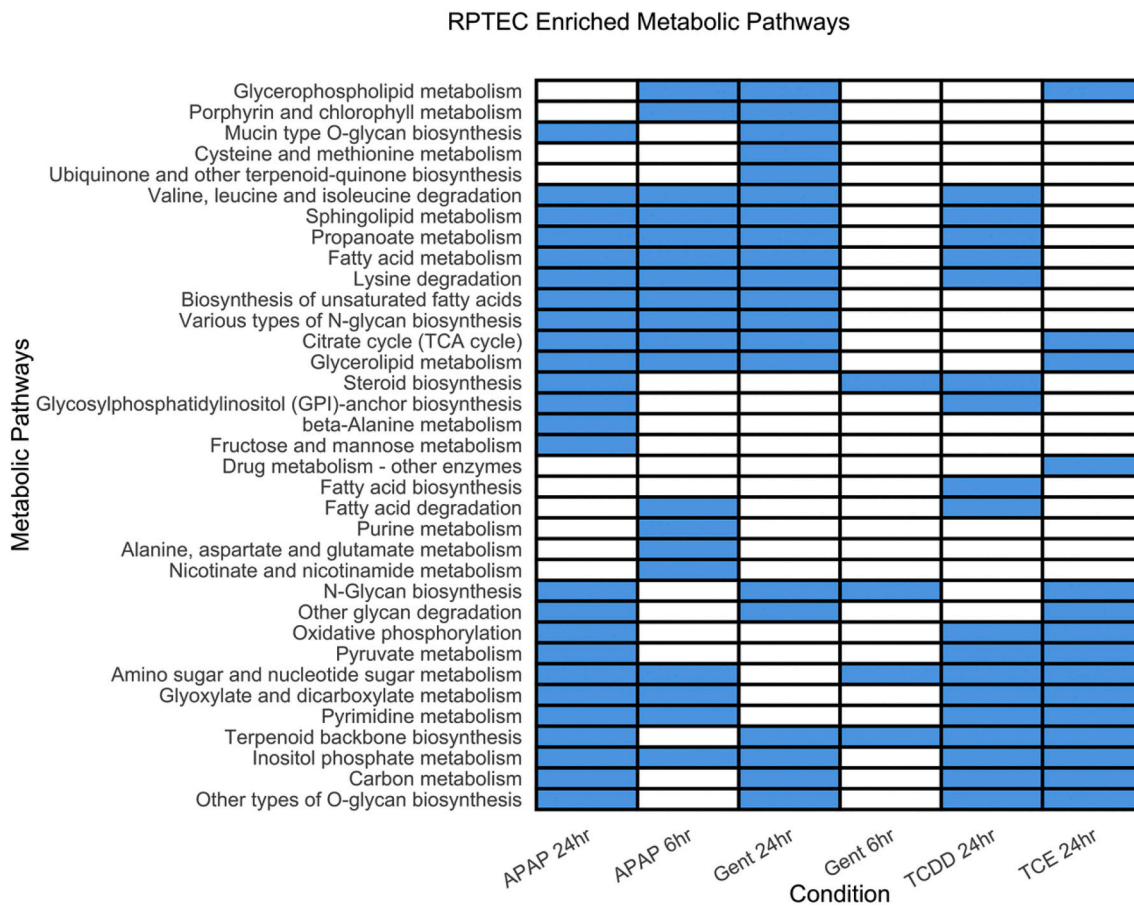


**Fig. 3.** Enriched metabolic pathways in response to toxicant exposure.

For the conditions for which there were enough differentially expressed genes, KEGG pathway enrichment is shown with blue indicating that a pathway is enriched, and white showing that pathways were not enriched. A select number of KEGG metabolic pathways are displayed on the y-axis, with experimental conditions listed on the x-axis. Pathways are clustered by Euclidean distance using complete linkage. Dendrogram not shown.

**Table 2**

Number of metabolite levels that were differentially changed compared to DMSO controls, and how many of those metabolites are accounted for in the *iRno* network reconstruction. Changes in metabolite levels are considered statistically significant if the normalized value was different from DMSO controls at the BH-adjusted *p*-value < 0.1.

Chemical Compound	Statistically significant changes in metabolite levels	The subset of statistically significant changes in metabolite levels that map to <i>iRno</i>
APAP – 6 h	5	4
APAP – 24 h	5	5
Gent – 6 h	4	3
Gent – 24 h	1	1
TCDD – 6 h	4	3
TCDD – 24 h	2	2
TCE – 6 h	1	1
TCE – 24 h	1	1

identify.

### 3.5. Transcriptomics and metabolomics data suggest different responses to compound exposure

After separately analyzing the transcriptomics data and the metabolomics data, we then interrogated the data together to identify consistencies and inconsistencies. Given that we observed a significant increase in glycine compared to the control groups in the metabolomics data (Fig. 4), we identified reactions from *iRno* that contained glycine

and determined if the genes associated with these reactions were differentially expressed. We see increased gene expression for a number of transporters involved in glycine transport for the APAP, Gent, and TCDD conditions at 24 h (*Slc7a5*, *Slc3a2*, *Slc36a1*). Next, we see the gene *Shmt1*, which catalyzes a reaction in the glycine, serine, and threonine metabolism subsystem, is differentially expressed for the APAP, Gent, and TCDD conditions at 24 h. Finally, we see the gene *Sirt3*, a sirtuin involved in metabolic regulation but that also catalyzes a reaction in the aromatic amino acid subsystem, is differentially expressed in the APAP, Gent, and TCDD conditions at 24 h. In addition, a number of other genes that catalyzed reactions involving glycine were uniquely differentially expressed between the APAP, Gent and TCDD conditions at 24 h. However, all of the common genes were not uniquely differentially expressed in the APAP, Gent, and TCDD conditions at 24 h even though we only measured a statistically significant increase in glycine in the metabolomics data for these conditions. Together with the number of unique differentially expressed genes for each of these three conditions identified with the *iRno* model, this suggests unique pathways in each condition may be contributing to glycine production. This highlights the need for pathway-level analyses to identify genes or reactions driving the measured changes in the metabolomics data.

### 3.6. *iRno* predicts changes in metabolites observed by the omics data

To make predictions on metabolite level changes, we used our updated *iRno* model and the transcriptomics data along with the Transcriptionally Inferred Metabolite Biomarker Response (TIMBR) algorithm (Blais et al. 2017). TIMBR overlays gene expression fold changes

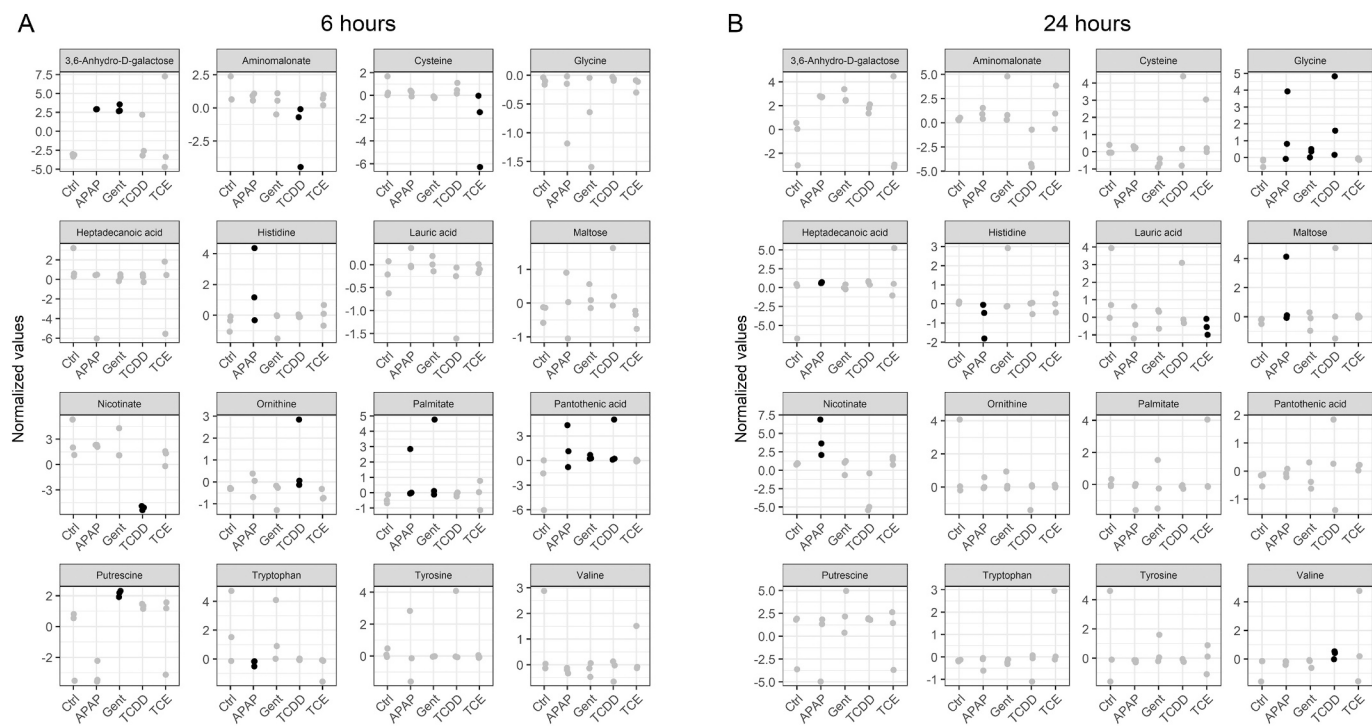


**Fig. 4.** Changes in secreted metabolite levels in response to toxicant exposure.

The dotplots above show the metabolomics data after normalization for both six (A) and twenty four (B) hours. Each data point indicates a separate well replicate where three wells were run for experimental condition. For each data point, normalized metabolite abundances from blank media were subtracted to show positive values indicating a metabolite was produced, and negative values indicating a metabolite was consumed. The sixteen metabolites shown are those that were statistically changed in one of the five experimental conditions compared to blank media or the DMSO control samples. Black dots indicate a statistical change from the control condition (Kruskal-Wallis,  $p$ -value  $< 0.05$ ).

on the network and applies corresponding weights to metabolic reactions in the model. For each metabolite that can be produced in the model, TIMBR then minimizes the sum of fluxes for a treatment and a control case to determine a metabolite's availability to be produced from the model. Overall, we were able to make TIMBR predictions for APAP and Gent at the six-hour timepoint, and APAP, Gent, TCDD, and TCE at the 24-h timepoint for a total of 245 metabolites, based on differentially expressed genes at each of these conditions. Raw TIMBR production scores are displayed in Supplementary Data 4.

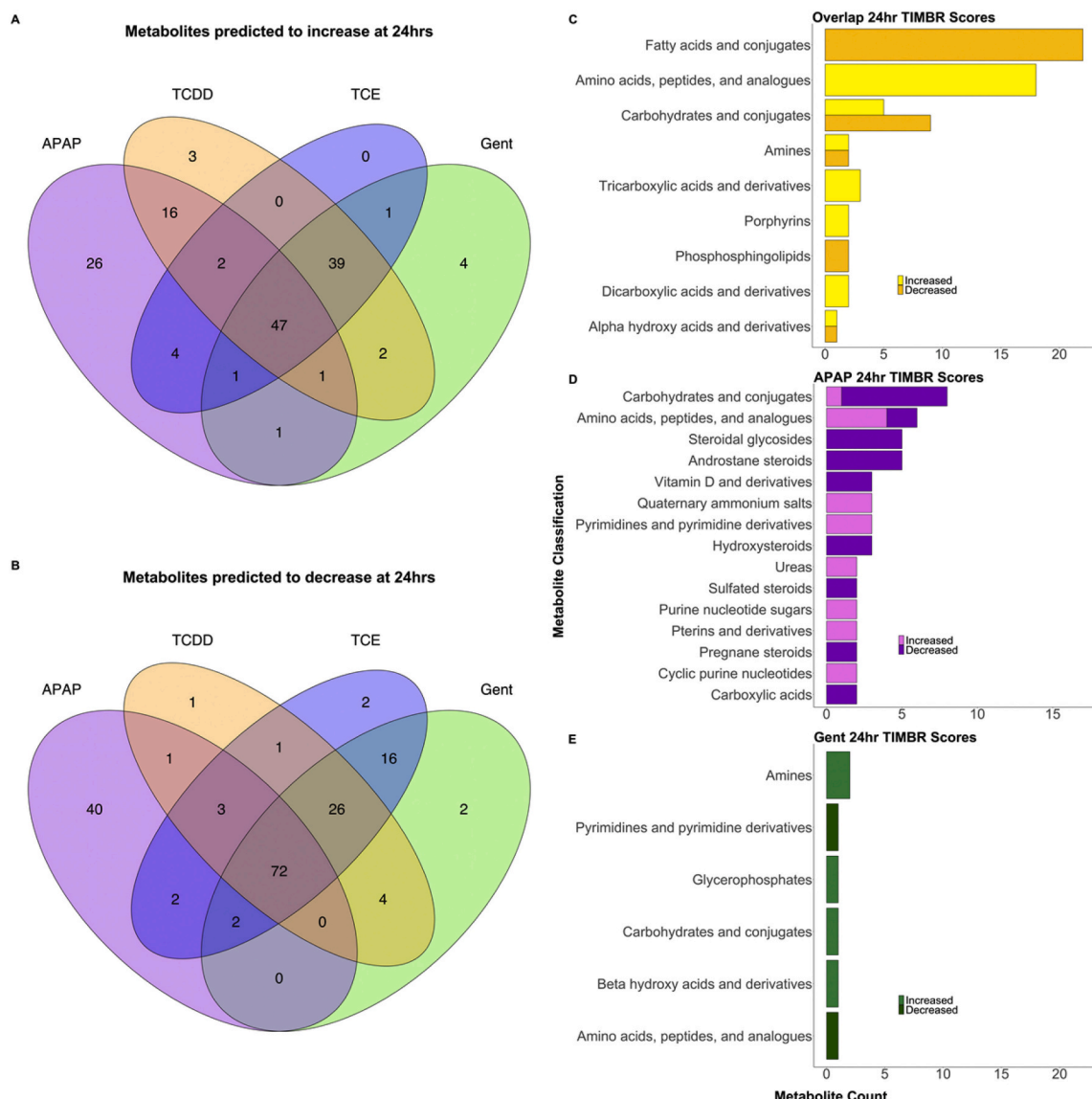
Fig. 5 shows the number of metabolites predicted to increase or decrease at the 24-h timepoint. At the 24-h timepoint, increases in 47 metabolites and decreases in 72 metabolites were predicted in production across all conditions (APAP, Gent, TCDD, and TCE). For this timepoint, amino acids were predicted to increase in response to treatment, which was contradictory to what we saw at the six-hour timepoint. One example of this difference is with serine, as it was predicted to increase at 24 h and was predicted to decrease at six hours. The increase in serine could support the idea that gluconeogenesis is inhibited, where the increase in serine could be due to the conversion of glutamine and glutamate to serine (van de Poll et al. 2004). At the 24-h timepoint, fatty acids and conjugates were the largest group predicted to decrease across all compounds. The decrease in fatty acids and conjugates could potentially point to the use of fatty acids as an energy source during stress, instead of amino acids which were predicted to increase in production across all compounds at 24 h. The proximal tubules mostly reabsorb filtered amino acids (Dantzler and Silbernagl 1988), so this predicted increase in amino acid production could be an indication of altered transport of amino acids under the *in vitro* tested conditions.

We next looked at compound-specific responses to see if there were other aspects of RPTEC metabolism that were altered. At the six-hour timepoint, APAP was predicted to cause a decrease in the production of amino acids and analogs and an increase in the production in

carbohydrate compounds contrary to what we predicted at the 24-h timepoint. For Gent at the six-hour time-point, amino acids and analogs were predicted to increase, similar to the general trend we predicted at the 24-h timepoint. Fatty acids were predicted to decrease, which also agrees with the general trend we noticed at the 24-h timepoint. Fatty acid oxidation inhibits glycolysis and increases enzyme activity of gluconeogenesis (Owen et al. 1969), so this decrease further supports the breakdown of the production of glucose by allowing glycolysis to proceed. These results highlight the utility of using the model to further investigate the changes in metabolism measured by transcriptomics and predicting how metabolism proceeds in proximal tubule cells in response to xenobiotics.

#### 4. Discussion

The kidneys are highly metabolically active (Gallagher et al. 2006). While we have a general understanding of kidney function, more information is needed on exactly how they lose function as well as indicators of declining function. One advantage of computational models is that they can be used to investigate biological changes or emergent phenomena of a particular biological system that could arise from perturbations to the surrounding environment. GENREs have emerged as useful tools to help point specifically to genes or proteins of interest associated with observed phenotypic changes or to characterize the overall response to an altered state of the system. To date, GENREs that represent kidney function have been limited in size and coverage of metabolic pathways, and some networks have been created to study a particular disease. Here, we present an update to an existing model of rat metabolism (Blais et al. 2017) that is validated for kidney function. Additionally, we profiled the metabolic responses of RPTECs exposed to a broad range of compounds of different classifications and used our model to assess some of the measured metabolic changes. The analysis

**Fig. 5.** Summary of TIMBR production scores.

Venn diagrams show the number of metabolites that were predicted to increase (A) or decrease (B) after exposure to APAP, Gent, TCDD, or TCE after twenty four hours. Bar charts show Human Metabolome DataBase classifications for metabolites that overlap (C), APAP (D), and Gent (E) for twenty four hours.

exhibits the utility of our model by predicting changes in metabolism that can be compared with experimental data. Importantly, demonstrating how *iRno* can be used with multiple types of experimental datasets to identify how metabolic pathways are linked to compound exposure.

We have added new objective functions to *iRno* to include a generic biomass function for non-liver cells and to capture functions specific to kidney metabolism. First, we used the model to simulate gluconeogenesis from lactate, glutamine, and glycerol precursors. Additionally, we looked at genes necessary for gluconeogenesis from the available precursors and found that 22 genes related to either ATP synthase or cytochrome c oxidase were necessary to produce glucose. Since gluconeogenesis requires ATP for completion (Ross et al. 1986), the cytochrome c oxidase genes would also be necessary as they are involved in the generation of ATP (Fontanesi et al. 2006). For the new biomass equation, we found that sixteen genes were no longer required to synthesize biomass. These genes belong to the Cyp450 family (e.g., *Cyp27a1*, *Cyp3a18*) and also included genes that are involved in the reduction or oxidation of steroids and fatty acids (e.g., *Acaa1*, *Akr1c14*, *Akr1d1*, *Amacr*), which are necessary for bile acid synthesis (Chiang 2013; Šarenac and Mikov 2018).

In order to better understand the response of the kidneys to different compounds, we profiled RPTECs exposed to both pharmaceutical and environment compounds. Across all compounds, we highlight differential metabolic genes for both amino acid and fatty acid metabolism that are shared across compounds. While some previously identified biomarkers for kidney injury did not appear in the profiling data (e.g., KIM-1 (Vaidya et al. 2010)), other markers were identified (e.g., Clusterin). These discrepancies could be a function of *in vitro* vs. *in vivo* experimental conditions, compound concentrations, or time points, among others. It is important to consider how differences in such parameters could affect the detection and validity of such biomarkers.

From the metabolomics data, we noted varied changes in amino acid levels in response to the compounds, particularly in the production of glycine at 24 h. While glycine is measured to be changed in production, we identified few common changes in the differentially expressed genes mapping to reactions involving glycine. This highlights the complexity of the relationship between differential expression and metabolism and the utility of models in reconciling these observed differences. When integrating our collected transcriptomics data with the *iRno* model, amino acids were consistently predicted to be increased as a result of

treatment at the 24-h timepoint across all conditions and in Gent at six hours. For the APAP condition, TCA cycle metabolites increase at the six-hour timepoint. This difference to other studies could be due a lack of assessment at the early exposure of compounds to the renal system or differences between compounds used to assess nephrotoxicity.

One limitation of this study is that there is a small number of metabolites that overlap between the metabolomics data and the model. While we can still learn about general trends in metabolism from the paired omics datasets, this study could go further by validating predictions of changes in the metabolite levels at six hours to support studying changes in kidney metabolism earlier than 24 h. The *iRno* network reconstruction can be further curated to include more genes and metabolic reactions to capture more areas of metabolism. As our knowledge of kidney biological function expands, the model will also expand to better account for rat kidney metabolism. Currently, we are successfully able to capture some changes in kidney metabolism and to use the model to make predictions on the changes in metabolism associated with compounds representative of both intentional exposures (e.g. pharmaceuticals: acetaminophen and gentamicin) and unintentional exposures (e.g. environmental: TCE and TCDD). The ability to capture these changes in kidney metabolism is useful for understanding indicators of declining kidney function prior to injury, but could also be further developed as a method to validate known nephrotoxic drugs as well as identify candidate drugs with potential nephrotoxic effects. Extensive open source datasets such as TG-GATES and Drug Matrix are well suited to use in the platform presented here and targeted predictions can be validated using appropriate experimental systems (Blais et al. 2017). Our approach for using a GENRE with paired omics data provides a holistic approach to identify and understand declining kidney function.

## Author contributions

KR, GK, AW, and JP participated in study conceptualization. KR, GK, and BD conducted methodology. KR performed formal analysis, while KR and BD carried out data visualization. KR wrote the initial draft of the manuscript. KR, BD, GK, VP, KV, AW, and JP reviewed and edited the final manuscript.

## Declaration of Competing Interest

The authors declare that they have no conflict of interest.

## Acknowledgments

Support for this project was provided by the United States Department of Defense (W81XWH-14-C-0054 to JP). The opinions and assertions contained herein are the private views of the authors and are not to be construed as the official or as reflecting the views of the U.S. Army, the U.S. Department of Defense, or the Henry M. Jackson Foundation for the Advancement of Military Medicine, Inc. (HJF). This manuscript has been approved for public release with unlimited distribution.

## Appendix A. Supplementary data

The raw RNA sequencing and processed data discussed in this publication have been deposited in NCBI's Gene Expression Omnibus, GSE 141628 (Edgar et al. 2002). Supplementary Data 1 provides a summary of changes to the *iRno* model while Supplementary Data 2 provides the updated model in sbml format. Spreadsheets for differentially expressed genes and enrichR gene enrichment results are included in Supplementary Data 3 and Supplementary Data 4, respectively. Metabolomics data and analysis are available in Supplementary Data 5. TIMBR production scores are available in Supplementary Data 6. Supplementary Data 7 provides annotations to uniquely increased or decreased TIMBR production scores for each condition, and Supplementary Data 8

provides gene inputs and reaction outputs for the iMAT model created to run TIMBR predictions.

## References

- Adiyanti, S.S., Loho, T., 2012. Acute kidney injury (AKI) biomarker. *Acta Med. Indones.* 44 (3), 246–255.
- Agren, R., Mardinoglu, A., Asplund, A., Kampf, C., Uhlen, M., Nielsen, J., 2014. Identification of anticancer drugs for hepatocellular carcinoma through personalized genome-scale metabolic modeling. *Mol. Syst. Biol.* 10, 721. <https://doi.org/10.1002/msb.145122>.
- Banday, A.A., Farooq, N., Priyamvada, S., Yusufi, A.N.K., Khan, F., 2008. Time dependent effects of gentamicin on the enzymes of carbohydrate metabolism, brush border membrane and oxidative stress in rat kidney tissues. *Life Sci.* 82 (9–10), 450–459. <https://doi.org/10.1016/j.lfs.2007.11.014>.
- Bartell, J.A., Blazier, A.S., Yen, P., Thøgersen, J.C., Jelsbak, L., Goldberg, J.B., Papin, J. A., 2017. Reconstruction of the metabolic network of *Pseudomonas aeruginosa* to interrogate virulence factor synthesis. *Nat. Commun.* 8, 14631. <https://doi.org/10.1038/ncomms14631>.
- Baud, L., Ardaillou, R., 1986. Reactive oxygen species: production and role in the kidney. *Am. J. Phys.* 251 (5 Pt 2), F765–F776. <https://doi.org/10.1152/ajprenal.1986.251.5.F765>.
- Bellomo, R., Kellum, J.A., Ronco, C., 2012. Acute kidney injury. *Lancet* 380 (9843), 756–766. [https://doi.org/10.1016/S0140-6736\(11\)61454-2](https://doi.org/10.1016/S0140-6736(11)61454-2).
- Bentli, R., Ciftci, O., Cetin, A., Unlu, M., Basak, N., Cay, M., 2013. Oral administration of hesperidin, a citrus flavonone, in rats counteracts the oxidative stress, the inflammatory cytokine production, and the hepatotoxicity induced by the ingestion of 2,3,7,8-tetrachlorodibenzo-p-dioxin (TCDD). *Eur. Cytokine Netw.* 24 (2), 91–96. <https://doi.org/10.1684/ecri.2013.0337>.
- Blais, E.M., Rawls, K.D., Dougherty, B.V., Li, Z.I., Kolling, G.L., Ye, P., Wallqvist, A., Papin, J.A., 2017. Reconciled rat and human metabolic networks for comparative toxicogenomics and biomarker predictions. *Nat. Commun.* 8, 14250. <https://doi.org/10.1038/ncomms14250>.
- Blanchet, L., Smolinska, A., Attali, A., Stoop, M.P., Ampt, K.A., van Aken, H., Suijgeest, E., Tuinstra, T., Wijmenga, S.S., Luider, T., et al., 2011. Fusion of metabolomics and proteomics data for biomarkers discovery: case study on the experimental autoimmune encephalomyelitis. *BMC Bioinform.* 12 (1). <https://doi.org/10.1186/1471-2105-12-254> [accessed 2019 Oct 29]. <https://bmcbioinformatics.biomedcentral.com/articles/10.1186/1471-2105-12-254>.
- Booblescu, I.A., 2010. Renal lipid metabolism and lipotoxicity. *Curr. Opin. Nephrol. Hypertens.* 19 (4), 393–402. <https://doi.org/10.1097/MNH.0b013e32833aa4ac>.
- Bonventre, J.V., 2014. Kidney injury molecule-1: a translational journey. *Trans. Am. Clin. Climatol. Assoc.* 125, 293–299 (discussion 299).
- Boogaard, P.J., Mulder, G.J., Nagelkerke, J.F., 1989. Isolated proximal tubular cells from rat kidney as an in vitro model for studies on nephrotoxicity. *Toxicol. Appl. Pharmacol.* 101 (1), 144–157. [https://doi.org/10.1016/0041-008X\(89\)90220-2](https://doi.org/10.1016/0041-008X(89)90220-2).
- Boverhof, D.R., Burgoon, L.D., Tashiro, C., Sharratt, B., Chittim, B., Harkema, J.R., Mendrick, D.L., Zacharewski, T.R., 2006. Comparative toxicogenomic analysis of the hepatotoxic effects of TCDD in Sprague Dawley rats and C57BL/6 mice. *Toxicol. Sci.* 94 (2), 398–416. <https://doi.org/10.1093/toxsci/kfl100>.
- Bray, N.L., Pimentel, H., Melsted, P., Pachter, L., 2016. Near-optimal probabilistic RNA-seq quantification. *Nat. Biotechnol.* 34 (5), 525–527. <https://doi.org/10.1038/nbt.3519>.
- Cajka, T., Fiehn, O., 2017. LC-MS-based Lipidomics and automated identification of lipids using the LipidBlast in-Silico MS/MS library. *Methods Mol. Biol.* Clifton NJ. 1609, 149–170. [https://doi.org/10.1007/978-1-4939-6996-8\\_14](https://doi.org/10.1007/978-1-4939-6996-8_14).
- Canayakin, D., Bayir, Y., Kilic Baygutalp, N., Sezen Karaoglan, E., Atmaca, H.T., Kocak Ozgeris, F.B., Keles, M.S., Halici, Z., 2016. Paracetamol-induced nephrotoxicity and oxidative stress in rats: the protective role of *Nigella sativa*. *Pharm. Biol.* 54 (10), 2082–2091. <https://doi.org/10.3109/13880209.2016.1145701>.
- Carey, M.A., Papin, J.A., Guler, J.L., 2017. Novel plasmodium falciparum metabolic network reconstruction identifies shifts associated with clinical antimalarial resistance. *BMC Genomics* 18 (1), 543. <https://doi.org/10.1186/s12864-017-3905-1>.
- Chang, R.L., Lei, Xie, Bourne, P.E., Palsson, B.O., 2010. Drug off-target effects predicted using structural analysis in the context of a metabolic network model. Dunbrack RL, ed. *PLoS Comput. Biol.* 6 (9), e1000938 <https://doi.org/10.1371/journal.pcbi.1000938>.
- Chiang, J.Y.L., 2013. Bile acid metabolism and signaling. *Compr. Physiol.* 3 (3), 1191–1212. <https://doi.org/10.1002/cphy.c120023>.
- Cojocel, C., Beuter, W., Müller, W., Mayer, D., 1989. Lipid peroxidation: a possible mechanism of trichloroethylene-induced nephrotoxicity. *Toxicology* 55 (1–2), 131–141. [https://doi.org/10.1016/0300-483X\(89\)90180-7](https://doi.org/10.1016/0300-483X(89)90180-7).
- Connor, S.C., Hansen, M.K., Corner, A., Smith, R.F., Ryan, T.E., 2010. Integration of metabolomics and transcriptomics data to aid biomarker discovery in type 2 diabetes. *Mol. BioSyst.* 6 (5), 909. <https://doi.org/10.1039/b914182k>.
- Dantzler, W.H., Silbermagl, S., 1988. Amino acid transport by juxtaglomerular nephrons: distal reabsorption and recycling. *Am. J. Phys.* 255 (3 Pt 2), F397–F407. <https://doi.org/10.1152/ajprenal.1988.255.3.F397>.
- Dieterle, F., Perentes, E., Cordier, A., Roth, D.R., Verdes, P., Grenet, O., Pantano, S., Moulin, P., Wahl, D., Mahl, A., et al., 2010. Urinary clusterin, cystatin C, beta2-microglobulin and total protein as markers to detect drug-induced kidney injury. *Nat. Biotechnol.* 28 (5), 463–469. <https://doi.org/10.1038/nbt.1622>.
- Dong, B., Nishimura, N., Vogel, C.F., Tohyama, C., Matsumura, F., 2010. TCDD-induced cyclooxygenase-2 expression is mediated by the nongenomic pathway in mouse

- MMDD1 macula densa cells and kidneys. *Biochem. Pharmacol.* 79 (3), 487–497. <https://doi.org/10.1016/j.bcp.2009.08.031>.
- Edgar, R., Domrachev, M., Lash, A.E., 2002. Gene expression omnibus: NCBI gene expression and hybridization array data repository. *Nucleic Acids Res.* 30 (1), 207–210. <https://doi.org/10.1093/nar/30.1.207>.
- Elhamri, M., Martin, M., Ferrier, B., Baverel, G., 1993. Substrate uptake and utilization by the kidney of fed and starved rats *in vivo*. *Ren. Physiol. Biochem.* 16 (6), 311–324.
- Endre, Z.H., Pickering, J.W., Walker, R.J., Devarajan, P., Edelstein, C.L., Bonventre, J.V., Frampton, C.M., Bennett, M.R., Ma, Q., Sabbisetti, V.S., et al., 2011. Improved performance of urinary biomarkers of acute kidney injury in the critically ill by stratification for injury duration and baseline renal function. *Kidney Int.* 79 (10), 1119–1130. <https://doi.org/10.1038/ki.2010.555>.
- Fiehn, O., 2016. Metabolomics by gas chromatography-mass spectrometry: combined targeted and untargeted profiling. *Curr. Protoc. Mol. Biol.* 114, 30.4.1–30.4.32. <https://doi.org/10.1002/0471142727.mbb3004s114>.
- Fontanesi, F., Soto, I.C., Horn, D., Barrientos, A., 2006. Assembly of mitochondrial cytochrome c -oxidase, a complicated and highly regulated cellular process. *Am. J. Physiol.-Cell Physiol.* 291 (6), C1129–C1147. <https://doi.org/10.1152/ajpcell.00233.2006>.
- Gallagher, D., Albu, J., He, Q., Heshka, S., Boxt, L., Krasnow, N., Elia, M., 2006. Small organs with a high metabolic rate explain lower resting energy expenditure in African American than in white adults. *Am. J. Clin. Nutr.* 83 (5), 1062–1067. <https://doi.org/10.1093/ajcn/83.5.1062>.
- Gerich, J.E., Meyer, C., Woerle, H.J., Stumvoll, M., 2001. Renal gluconeogenesis: its importance in human glucose homeostasis. *Diabetes Care* 24 (2), 382–391. <https://doi.org/10.2337/diacare.24.2.382>.
- de Geus, H.R.H., Betjes, M.G., Bakker, J., 2012. Biomarkers for the prediction of acute kidney injury: a narrative review on current status and future challenges. *Clin. Kidney J.* 5 (2), 102–108. <https://doi.org/10.1093/ckj/sfs008>.
- Gowda, S., Desai, P.B., Kulkarni, S.S., Hull, V.V., Math, A.A.K., Vernekar, S.N., 2010. Markers of renal function tests. *North Am J Med Sci* 2 (4), 170–173.
- Griffin, B.R., Faubel, S., Edelstein, C.L., 2019. Biomarkers of drug-induced kidney toxicity. *Ther. Drug Monit.* 41 (2), 213–226. <https://doi.org/10.1097/FTD.0000000000000589>.
- Himmelfarb, J., Ikizler, T.A., 2007. Acute kidney injury: changing lexicography, definitions, and epidemiology. *Kidney Int.* 71 (10), 971–976. <https://doi.org/10.1038/sj.ki.5002224>.
- Kim, S.Y., Moon, A., 2012. Drug-induced nephrotoxicity and its biomarkers. *Biomol. Ther.* 20 (3), 268–272. <https://doi.org/10.4062/biomolther.2012.20.3.268>.
- Lash, L.H., Qian, W., Putt, D.A., Hueni, S.E., Elfarra, A.A., Krause, R.J., Parker, J.C., 2001. Renal and hepatic toxicity of trichloroethylene and its glutathione-derived metabolites in rats and mice: sex-, species-, and tissue-dependent differences. *J. Pharmacol. Exp. Ther.* 297 (1), 155–164.
- Layton, A.T., 2013. Mathematical modeling of kidney transport. *Wiley Interdiscip. Rev. Syst. Biol. Med.* 5 (5), 557–573. <https://doi.org/10.1002/wsbm.1232>.
- Love, M.I., Huber, W., Anders, S., 2014. Moderated estimation of fold change and dispersion for RNA-seq data with DESeq2. *Genome Biol.* 15 (12), 550. <https://doi.org/10.1186/s13059-014-0550-8>.
- Luo, Q.-H., Chen, M.-L., Chen, Z.-L., Huang, C., Cheng, A.-C., Fang, J., Tang, L., Geng, Y., 2016. Evaluation of KIM-1 and NGAL as early indicators for assessment of gentamycin-induced nephrotoxicity *in vivo* and *in vitro*. *Kidney Blood Press. Res.* 41 (6), 911–918. <https://doi.org/10.1159/000452592>.
- Mardinoglu, A., Agren, R., Kampf, C., Asplund, A., Uhlen, M., Nielsen, J., 2014. Genome-scale metabolic modelling of hepatocytes reveals serine deficiency in patients with non-alcoholic fatty liver disease. *Nat. Commun.* 5, 3083. <https://doi.org/10.1038/ncomms4083>.
- Matheis, K.A., Com, E., Gautier, J.-C., Guerreiro, N., Brandenburg, A., Gmuender, H., Sposny, A., Hewitt, P., Ambberg, A., Boernsen, O., et al., 2011. Cross-study and cross-omics comparisons of three nephrotoxic compounds reveal mechanistic insights and new candidate biomarkers. *Toxicol. Appl. Pharmacol.* 252 (2), 112–122. <https://doi.org/10.1016/j.taap.2010.11.006>.
- Matyash, V., Liebisch, G., Kurzchalia, T.V., Shevchenko, A., Schwudke, D., 2008. Lipid extraction by methyl-tert-butyl ether for high-throughput lipidomics. *J. Lipid Res.* 49 (5), 1137–1146. <https://doi.org/10.1194/jlr.D700041-JLR200>.
- Mazer, M., Perrone, J., 2008. Acetaminophen-induced nephrotoxicity: pathophysiology, clinical manifestations, and management. *J. Med. Toxicol.* 4 (1), 2–6. <https://doi.org/10.1007/BF03160941>.
- Meissen, J.K., Hirahatake, K.M., Adams, S.H., Fiehn, O., 2015. Temporal metabolic responses of cultured HepG2 liver cells to high fructose and high glucose exposures. *Metabol. Off. J. Metabol. Soc.* 11 (3), 707–721. <https://doi.org/10.1007/s11306-014-0729-8>.
- Mugford, C., 1997. The contribution of oxidation and deacetylation to acetaminophen nephrotoxicity in female Sprague-Dawley rats. *Toxicol. Lett.* 93 (1), 15–22. [https://doi.org/10.1016/S0378-4274\(97\)00063-5](https://doi.org/10.1016/S0378-4274(97)00063-5).
- Narayana, K., 2008. An aminoglycoside antibiotic gentamycin induces oxidative stress, reduces antioxidant reserve and impairs spermatogenesis in rats. *J. Toxicol. Sci.* 33 (1), 85–96. <https://doi.org/10.2131/jts.33.85>.
- Newton, J.F., Yoshimoto, M., Bernstein, J., Rush, G.F., Hook, J.B., 1983. Acetaminophen nephrotoxicity in the rat. *Toxicol. Appl. Pharmacol.* 69 (2), 291–306. [https://doi.org/10.1016/0041-008X\(83\)90311-3](https://doi.org/10.1016/0041-008X(83)90311-3).
- Nguan, C.Y.C., Guan, Q., Gleave, M.E., Du, C., 2014. Promotion of cell proliferation by clusterin in the renal tissue repair phase after ischemia-reperfusion injury. *Am. J. Physiol.-Ren. Physiol.* 306 (7), F724–F733. <https://doi.org/10.1152/ajprenal.00410.2013>.
- O'Brien, E.J., Monk, J.M., Palsson, B.O., 2015. Using genome-scale models to predict biological capabilities. *Cell.* 161 (5), 971–987. <https://doi.org/10.1016/j.cell.2015.05.019>.
- Ogle, D.H., Wheeler, P., Dinno, A., 2019. FSA: Fisheries Stock Analysis. <https://github.com/droglen/FSA>.
- Onopiuk, A., Tokarzewicz, A., Gorodkiewicz, E., 2015. Cystatin C. In: *Advances in Clinical Chemistry*, vol. 68. Elsevier, pp. 57–69 [accessed 2019 Oct 29]. <https://linkinghub.elsevier.com/retrieve/pii/S0065242314000389>.
- Orth, J.D., Conrad, T.M., Na, J., Lerman, J.A., Nam, H., Feist, A.M., Palsson, B.O., 2011. A comprehensive genome-scale reconstruction of Escherichia coli metabolism—2011. *Mol. Syst. Biol.* 7, 535. <https://doi.org/10.1038/msb.2011.65>.
- Owen, O.E., Felig, P., Morgan, A.P., Wahren, J., Cahill, G.F., 1969. Liver and kidney metabolism during prolonged starvation. *J. Clin. Invest.* 48 (3), 574–583. <https://doi.org/10.1172/JCI106016>.
- Pannala, V.R., Vinnakota, K.C., Rawls, K.D., Estes, S.K., O'Brien, T.P., Printz, R.L., Papin, J.A., Reifman, J., Shiota, M., Young, J.D., et al., 2019. Mechanistic identification of biofluid metabolite changes as markers of acetaminophen-induced liver toxicity in rats. *Toxicol. Appl. Pharmacol.* 372, 19–32. <https://doi.org/10.1016/j.taap.2019.04.001>.
- van de Poll, M.C., Soeters, P.B., Deutz, N.E., Fearon, K.C., Dejong, C.H., 2004. Renal metabolism of amino acids: its role in interorgan amino acid exchange. *Am. J. Clin. Nutr.* 79 (2), 185–197. <https://doi.org/10.1093/ajcn/79.2.185>.
- Ratliff, B.B., Abdulkhalid, W., Pawar, R., Wolin, M.S., 2016. Oxidant mechanisms in renal injury and disease. *Antioxid. Redox Signal.* 25 (3), 119–146. <https://doi.org/10.1089/ars.2016.6665>.
- Rawls, K.D., Blais, E.M., Dougherty, B.V., Vinnakota, K.C., Pannala, V.R., Wallqvist, A., Kolling, G.L., Papin, J.A., 2019a. Genome-scale characterization of toxicity-induced metabolic alterations in primary hepatocytes. *Toxicol. Sci. Off. J. Soc. Toxicol.* 172 (2), 279–291. <https://doi.org/10.1093/toxsci/kfz197>.
- Rawls, K.D., Dougherty, B.V., Blais, E.M., Stancliffe, E., Kolling, G.L., Vinnakota, K., Pannala, V.R., Wallqvist, A., Papin, J.A., 2019b. A simplified metabolic network reconstruction to promote understanding and development of flux balance analysis tools. *Comput. Biol. Med.* 105, 64–71. <https://doi.org/10.1016/j.combiomed.2018.12.010>.
- Robbiano, L., Baroni, D., Carrozzino, R., Mereto, E., Brambilla, G., 2004. DNA damage and micronuclei induced in rat and human kidney cells by six chemicals carcinogenic to the rat kidney. *Toxicology*. 204 (2–3), 187–195. <https://doi.org/10.1016/j.tox.2004.06.057>.
- Ross, B.D., Espinal, J., Silva, P., 1986. Glucose metabolism in renal tubular function. *Kidney Int.* 29 (1), 54–67. <https://doi.org/10.1038/ki.1986.20>.
- Särenäkki, T.M., Mikov, M., 2018. Bile acid synthesis: from nature to the chemical modification and synthesis and their applications as drugs and nutrients. *Front. Pharmacol.* 9 <https://doi.org/10.3389/fphar.2018.00939> [accessed 2019 Oct 30].
- Sawada, R., Iwata, M., Tabei, Y., Yamato, H., Yamanishi, Y., 2018. Predicting inhibitory and activatory drug targets by chemically and genetically perturbed transcriptome signatures. *Sci. Rep.* 8 (1) <https://doi.org/10.1038/s41598-017-18315-9> [accessed 2019 Oct 29].
- Schellenberger, J., Que, R., Fleming, R.M.T., Thiele, I., Orth, J.D., Feist, A.M., Zielinski, D.C., Bordbar, A., Lewis, N.E., Rahamanian, S., et al., 2011. Quantitative prediction of cellular metabolism with constraint-based models: the COBRA toolbox v2.0. *Nat. Protoc.* 6 (9), 1290–1307. <https://doi.org/10.1038/nprot.2011.308>.
- Scott, R.P., Quaggin, S.E., 2015. The cell biology of renal filtration. *J. Cell Biol.* 209 (2), 199–210. <https://doi.org/10.1083/jcb.201410017>.
- Sgouralis, I., Layton, A.T., 2015. Mathematical modeling of renal hemodynamics in physiology and pathophysiology. *Math. Biosci.* 264, 8–20. <https://doi.org/10.1016/j.mbs.2015.02.016>.
- Smith, J.H., 1988. The use of renal cortical slices from the Fischer 344 rat as an *in vitro* model to evaluate nephrotoxicity. *Fundam. Appl. Toxicol. Off. J. Soc. Toxicol.* 11 (1), 132–142. [https://doi.org/10.1016/0272-0590\(88\)90277-1](https://doi.org/10.1016/0272-0590(88)90277-1).
- Soga, T., Baran, R., Suematsu, M., Ueno, Y., Ikeda, S., Sakurakawa, T., Kakazu, Y., Ishikawa, T., Robert, M., Nishioka, T., et al., 2006. Differential metabolomics reveals ophthalmic acid as an oxidative stress biomarker indicating hepatic glutathione consumption. *J. Biol. Chem.* 281 (24), 16768–16776. <https://doi.org/10.1074/jbc.M610187200>.
- Sohrabi-Jahromi, S., Marashi, S.-A., Kalantari, S., 2016. A kidney-specific genome-scale metabolic network model for analyzing focal segmental glomerulosclerosis. *Mamm. Genome Off. J. Int. Mamm. Genome. Soc.* 27 (3–4), 158–167. <https://doi.org/10.1007/s00335-016-9622-2>.
- Soneson, C., Love, M.I., Robinson, M.D., 2015. Differential analyses for RNA-seq: transcript-level estimates improve gene-level inferences. *F1000Research*. 4, 1521. <https://doi.org/10.12688/f1000research.7563.2>.
- Spitzer, A., 1982. The role of the kidney in sodium homeostasis during maturation. *Kidney Int.* 21 (4), 539–545. <https://doi.org/10.1038/ki.1982.60>.
- Stempler, S., Yizhak, K., Ruppin, E., 2014. Integrating Transcriptomics with metabolic Modeling predicts biomarkers and drug targets for Alzheimer's disease. *Fong SS, editor PLoS One* 9 (8), e105383. <https://doi.org/10.1371/journal.pone.0105383>.
- Swainston, N., Smallbone, K., Hefzli, H., Dobson, P.D., Brewer, J., Hanscho, M., Zielinski, D.C., Ang, K.S., Gardiner, N.J., Gutierrez, J.M., et al., 2016. Recon 2.2: from reconstruction to model of human metabolism. *Metabolomics* 12 (7). <https://doi.org/10.1007/s11306-016-1051-4> [accessed 2018 Jun 26].
- Thiele, I., Swainston, N., Fleming, R.M.T., Hoppe, A., Sahoo, S., Aurich, M.K., Haraldsdottir, H., Mo, M.L., Rolfsson, O., Stobbe, M.D., et al., 2013. A community-driven global reconstruction of human metabolism. *Nat. Biotechnol.* 31 (5), 419–425. <https://doi.org/10.1038/nbt.2488>.

- Vaidya, V.S., Ferguson, M.A., Bonventre, J.V., 2008. Biomarkers of acute kidney injury. *Annu. Rev. Pharmacol. Toxicol.* 48, 463–493. <https://doi.org/10.1146/annurev.pharmtox.48.113006.094615>.
- Vaidya, V.S., Ozer, J.S., Frank, D., Collings, F.B., Ramirez, V., Troth, S., Muniappa, N., Thudium, D., Gerhold, D., Holder, D.J., et al., 2010. Kidney injury Molecule-1 outperforms traditional biomarkers of kidney injury in multi-site preclinical biomarker qualification studies. *Nat. Biotechnol.* 28 (5), 478–485. <https://doi.org/10.1038/nbt.1623>.
- Vrbová, M., Roušarová, E., Brůčková, L., Česla, P., Roušar, T., 2016. Characterization of acetaminophen toxicity in human kidney HK-2 cells. *Physiol. Res.* 65 (4), 627–635.
- Waikar, S.S., Bonventre, J.V., 2009. Creatinine kinetics and the definition of acute kidney injury. *J. Am. Soc. Nephrol.* 20 (3), 672–679. <https://doi.org/10.1681/ASN.2008070669>.
- Wang, J., Hou, Y., Duan, D., Zhang, Q., 2017. The structure and nephroprotective activity of oligo-porphyrin on glycerol-induced acute renal failure in rats. *Mar. Drugs.* 15 (5) <https://doi.org/10.3390/md15050135>.
- Weidemann, M.J., Krebs, H.A., 1969. The fuel of respiration of rat kidney cortex. *Biochem. J.* 112 (2), 149–166. <https://doi.org/10.1042/bj1120149>.
- Weinberg, J.M., Humes, H.D., 1980. Mechanisms of gentamicin-induced dysfunction of renal cortical mitochondria. I. Effects on mitochondrial respiration. *Arch. Biochem. Biophys.* 205 (1), 222–231. [https://doi.org/10.1016/0003-9861\(80\)90102-2](https://doi.org/10.1016/0003-9861(80)90102-2).
- Weinberg, J.M., Simmons, F., Humes, H.D., 1980. Alterations of mitochondrial respiration induced by aminoglycoside antibiotics. *Res. Commun. Chem. Pathol. Pharmacol.* 27 (3), 521–531.
- Yu, G., Wang, L.-G., Han, Y., He, Q.-Y., 2012. clusterProfiler: an R package for comparing biological themes among gene clusters. *OMICS J. Integr. Biol.* 16 (5), 284–287. <https://doi.org/10.1089/omi.2011.0118>.
- Zhang, A.-D., Dai, S.-X., Huang, J.-F., 2013. Reconstruction and analysis of human kidney-specific metabolic network based on Omics data. *Biomed. Res. Int.* 2013, 1–11. <https://doi.org/10.1155/2013/187509>.
- Zierer, J., Menni, C., Kastenmüller, G., Spector, T.D., 2015. Integration of ‘omics’ data in aging research: from biomarkers to systems biology. *Aging Cell* 14 (6), 933–944. <https://doi.org/10.1111/acel.12386>.